Optimization of Overcurrent Relay Coordination in a Radial Network Using the Adaptive Modified Firefly Algorithm for the EDG Blackstart System at Muara Tawar Combined Cycle Power Plant

Syaifur Ridzal, Dhany Harmeidy Barus
Master's Program in Electrical Engineering, Institut Teknologi PLN, Jakarta
E-mail: syaifurridzal2410735@itpln.ac.id, dhany@itpln.ac.id

Abstract—**Overcurrent relay (OCR) coordination in the radial EDG Blackstart system at the Muara Tawar Combined Cycle Power Plant is challenging because of the limited fault-current contribution of the synchronous generators. This study determines the optimal Time Dial Setting (TDS) using the Adaptive Modified Firefly Algorithm (AMFA) for five OCR setting groups, with R1 applied identically to the incoming relays of EDG1 and EDG2. The ETAP model produced a three-phase fault current of 823 A at R1 and 1645 A at R2 through R5. The pickup current was fixed at 249 A for R1 and 296.39 A for R2 through R5, while the MATLAB optimization used the IEC Normal Inverse characteristic and a minimum Coordination Time Interval (CTI) of 0.3 s. AMFA and PSO were evaluated over 30 runs with a population of 30 and 100 iterations. AMFA achieved a best fitness of 4.054961, a mean fitness of 4.081385, a sample standard deviation of 0.014481, a coefficient of variation of 0.35%, and a feasible rate of 100%. The best solution yielded TDS values of 0.2467, 0.2784, 0.2005, 0.1256, and 0.0500 for R1 through R5, respectively, with a total operating time of 4.054961 s. All CTIs satisfied the minimum limit, and the total operating time decreased by 62.88% compared with the existing settings. Compared with PSO, AMFA produced lower best and mean fitness values and smaller variation between runs. These results show that AMFA effectively accelerates and stabilizes OCR coordination for a fault at BUS33.**

Keywords—Adaptive Modified Firefly Algorithm, Coordination Time Interval, EDG Blackstart, Overcurrent Relay, Time Dial Setting.

I. INTRODUCTION

Power system protection is essential for maintaining the continuity and security of power-plant operations. In a power plant, a short-circuit fault may produce a substantial increase in current, damage equipment, and cause a wider outage if it is not isolated rapidly and selectively. Therefore, protection devices must be capable of detecting faults, issuing trip commands to circuit breakers, and isolating the faulted section without disrupting other healthy sections of the system.

The Jawa–Madura–Bali (JMB) system is the largest power system in Indonesia and supplies more than 75% of the national electricity demand; therefore, continuity of energy delivery within this system requires a high level of reliability [1]. A disturbance in the interconnected network may separate a subsystem from the main grid and cause it to operate in an islanded condition. Consequently, a fast and adaptive protection scheme is required to prevent subsystem operating failure [2].

One of the protection devices widely used in radial distribution systems is the Overcurrent Relay (OCR). An OCR operates according to the magnitude of the current flowing through the system. When the current exceeds the specified pickup value, the relay calculates its operating time based on the selected characteristic curve. For an OCR with an inverse characteristic, a higher fault current results in a shorter relay operating time. This characteristic is suitable for radial systems because it allows the relay closest to the fault location to operate first [3]. In isolated systems, non-adaptive OCR schemes with fixed settings are still used; therefore, their coordination is highly dependent on the operating condition for which the settings were established [4].

Coordination among OCRs is an important issue because the primary and backup relays must have an adequate operating-time margin. The difference between the operating times of the backup and primary relays is known as the Coordination Time Interval (CTI). If the CTI is too small, the backup relay may operate almost simultaneously with the primary relay, causing a wider outage. Conversely, an excessively large CTI delays fault clearing and may increase the risk of equipment damage. Therefore, the Time Dial Setting (TDS) must be determined optimally so that the relays operate rapidly while maintaining selectivity [3].

In practice, OCR settings are often determined conventionally through manual calculations and Time–Current Curve (TCC) analysis. This approach can serve as the basis for coordination, but it often requires an extensive trial-and-error process. Moreover, in systems where fault-current magnitudes at different locations are relatively close, a small change in TDS can significantly affect the CTI. This condition makes optimization methods relevant for obtaining improved settings. Previous studies have shown that OCR coordination optimization in radial networks with distributed generation must consider practical constraints so that minimum operating times remain selective [5], [6]. The integration of distributed generation may alter the short-circuit-current contribution observed by the relays and cause coordination problems if the settings are not adjusted [7].

Power-system reliability is improved not only by increasing generation capacity but also by reinforcing the network and developing the system configuration. A study of the Madura electrical subsystem showed that network reinforcement, the addition of local generation, and the development of a loop configuration can improve system resilience against disturbances [8]. From the protection perspective, the development of adaptive relays based on the IEC 61850 protocol can improve the ability of a

protection system to adjust its functions to changing operating conditions [9]. Adaptive protection schemes based on metaheuristic optimization have also been applied to improve the coordination of numerical and directional overcurrent relays under changing system conditions [10].

A conventional trial-and-error approach has limitations because it requires repeated evaluations and does not guarantee that the resulting setting combination is the best solution. In the standard Firefly Algorithm (FA), the random movement component may cause slow convergence and increase the risk of becoming trapped in a local optimum [11]. The AMFA study in the main reference [11] addressed this limitation in a radial system with distributed generation (DG); however, its application to an EDG Blackstart system using actual relay-setting data still requires formulation and validation specific to the system conditions. A modified firefly approach has also been applied to OCR coordination optimization [12]. In microgrids, OCR coordination optimization may also involve the TDS, pickup current, and selection of the characteristic curve, with PSO used as one of the solution methods [13].

The EDG Blackstart system at the Muara Tawar Combined Cycle Power Plant has distinctive characteristics because its sources are synchronous generators with limited capacity. Unlike a system directly connected to a large grid, the short-circuit-current contribution in the EDG system is relatively low. Consequently, the Plug Setting Multiplier (PSM) values observed by the relays may be relatively close, and the relay TCCs tend to be closely spaced. This condition presents a challenge for OCR coordination because the relays must continue to satisfy the minimum CTI despite the limited time margin between the curves.

This study uses the Adaptive Modified Firefly Algorithm (AMFA) as the primary method for optimizing the TDS values of five OCR setting groups. The R1 setting group is applied identically to the incoming relays of EDG1 and EDG2; therefore, the two relays are represented as one coordination stage with the same operating time. AMFA was selected because of its strong exploration capability and its ability to support the search for the best solution to a constrained nonlinear problem. To strengthen the evaluation, the AMFA results are compared in a limited manner with the existing relay settings and with Particle Swarm Optimization (PSO) as a benchmark method. Accordingly, the primary focus of this paper remains the application of AMFA, while PSO is used as an additional benchmark for evaluating solution quality.

The AMFA implementation in this study adopts the adaptive reduction of the randomization factor from the AMFA presented in the main reference [11], but it does not propose a new AMFA equation or algorithmic structure. The difference lies in the formulation and application object. Reference [11] optimized the plug setting and time setting multiplier of six OCRs in a radial system with DG under five operating conditions, whereas this study optimizes only the TDS values of five OCRs, maintains the pickup current as a fixed input based on the CT and relay data, and evaluates one three-phase fault scenario at BUS33 in the EDG Blackstart system of the Muara Tawar Combined Cycle Power Plant.

The contribution of this study is the application of AMFA to OCR coordination optimization in a radial EDG Blackstart system, the use of ETAP modeling data as the basis for the optimization inputs, and the evaluation of the results in terms of CTI, TCC, fitness, solution stability, and feasible rate. In addition, the existing relay settings are included as the initial condition and are compared with the optimization results, allowing the benefits of optimization to be evaluated in terms of improved coordination relative to the settings currently applied in the field.

Therefore, the novelty of this study is applicative and evaluative rather than the development of a new AMFA algorithm. It includes the integration of a field-data-based ETAP model with MATLAB optimization for an EDG Blackstart system, the use of a fixed pickup current so that the results can be applied to actual relay settings, reproducible verification of the PSM, operating time, and CTI, and a comparison of the existing settings, PSO, and AMFA over 30 runs. A specific approach is required because the EDG source has a limited fault-current level and the PSM values among the relays are relatively close; thus, small changes in TDS can affect the CTI, and coordination errors may disrupt the continuity of the blackstart restoration sequence.

II. Materials and Methods

A. Overcurrent Relay and IEC Normal Inverse Curve

An Overcurrent Relay is a protection relay that operates when the system current exceeds its pickup threshold. For an inverse-time OCR, the relay operating time is not constant but varies with the fault-current magnitude. The greater the fault current relative to the pickup current, the shorter the relay operating time. The relationship among fault current, pickup current, and relay operation is expressed through the Plug Setting Multiplier (PSM).

$$PSM = I_{fault} / I_{pickup}$$

This study uses the IEC Normal Inverse characteristic. This curve is widely applied in radial distribution systems because it provides relatively stable coordination characteristics over various fault-current levels. The relay operating time for the IEC Normal Inverse characteristic can be expressed as a function of TDS and PSM: $t = (0.14 \times TDS) / (PSM^{0.02} - 1)$. Based on this equation, TDS is the principal parameter that controls how rapidly or slowly the relay operates [14].

B. Coordination Time Interval and TCC

The Coordination Time Interval is the difference between the operating times of the backup and primary relays for the same fault location. In protection coordination, the primary relay must operate first because it is closest to the fault. The backup relay operates only if the primary relay fails to isolate the fault. Mathematically, the CTI is expressed as $CTI = t_{backup} - t_{primary}$.

In this study, the minimum CTI is set to 0.3 s and is used as the principal constraint in the optimization process. The Time-Current Curve (TCC) visualizes the relationship between fault current and relay operating time. In this paper, the existing relay TCC is used as the baseline and is

then compared with the TCC obtained from AMFA optimization.

C. *Research Object and Data*

The research object is the radial EDG Blackstart system at the Muara Tawar Combined Cycle Power Plant. The system is modeled using two synchronous generator units, EDG1 and EDG2, each rated at 2.5 MVA, 2.125 MW, 6.3 kV, and a power factor of 0.85. The system uses 6-kV Siemens NXAIR WORLD switchgear and Siemens SIPROTEC 5 series 7SJ82 relays for OCR protection [15].

The data used in this study include the single-line diagram, wiring diagram, CT data, relay data, existing relay settings, generator data, and cable data. Because detailed alternator data were not fully available, the generator reactance parameters were based on typical values for diesel synchronous generators. A subtransient reactance X″d of 0.15 pu was used as an important parameter for the three-phase short-circuit study.

Table I presents the generator parameters used as inputs to the ETAP model, particularly to represent source capacity and reactance characteristics in the load-flow and short-circuit studies.

TABLE I. GENERATOR DATA USED IN ETAP MODELING

Parameter	Value
Capacity	2.5 MVA
Active power	2.125 MW
Voltage	6.3 kV
Power factor	0.85
X″d	0.15 pu
X′d	0.25 pu
Xd	1.80 pu
X/R ratio	20

EDG1 was modeled as the swing bus, whereas EDG2 was modeled as a voltage-control or PV bus. In PV mode, EDG2 was assigned an active power of 2.125 MW with a voltage reference of 100%. Its reactive-power limits were set to +/-1.317 MVAr. This modeling approach is more realistic than assigning the entire load to the swing generator.

Table II presents the cable parameters that determine line impedance and current-carrying capacity in the system model.

TABLE II. CABLE DATA USED IN THE MODEL

Parameter	Value
Cable type	N2XSEYFGbY
Voltage	6/10 kV
Conductor material	Cu 3 x 300 mm²
Resistance	0.0601 ohm/km
Reactance	0.10 ohm/km
Length	1 km
Ground ampacity	532 A
Air ampacity	678 A

D. *ETAP Modeling*

The system was modeled in ETAP to obtain the normal operating condition and fault currents. Load-flow analysis was used to verify that the system configuration was technically feasible. In the analyzed scenario, only one main lumped load, Lump5, rated at 3 MVA with a nominal power factor of 0.85, was connected. The other loads were open and therefore did not absorb power in the load-flow results.

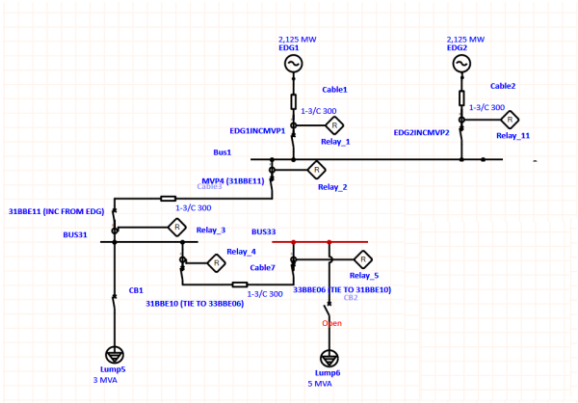


Fig. 1. Single-Line Diagram of the EDG Blackstart System at Muara Tawar Combined Cycle Power Plant

Fig1 is presented to show the radial network configuration, the positions of EDG1 and EDG2, the power-delivery path, and BUS33, which was selected as the fault location in this study.

Fig. 1 shows the system model used as the basis for all simulations, enabling the reader to understand the network configuration before the analysis is presented.

E. Load-Flow and Short-Circuit Simulations

The load-flow simulation was performed to validate bus voltages, power flows, and generator loading. The load-flow results were used to confirm that the system was in a normal operating condition before the short-circuit study was conducted. In addition, the load currents obtained from the load flow served as an initial reference for selecting the relay pickup currents so that the relays would not operate under normal conditions.

The load-flow results show different power-sharing characteristics for the two generators. EDG1 supplies 0.4436 MW and 1.5591 MVAr, whereas EDG2 supplies 2.1250 MW and 0.0481 MVAr. The apparent power and power factor of each generator were calculated using S = sqrt(P^2 + Q^2) and PF = P/S. The generator output, load, and system losses are summarized in Table V. According to the load-flow output, the current at EDG1INCMVP1 is 148.6 A, whereas that at EDG2INCMVP2 is 194.8 A. This difference results from the different active- and reactive-power sharing between EDG1 and EDG2.

Table III summarizes the normal operating currents from the load-flow analysis and the three-phase short-circuit currents observed by each circuit breaker for the BUS33 fault scenario.

TABLE III. LOAD-FLOW AND THREE-PHASE SHORT-CIRCUIT CURRENTS FOR THE BUS33 FAULT SCENARIO

No.	Circuit Breaker	Load-Flow Current (A)	Three-Phase Short-Circuit Current (A)
1	EDG1INCMVP1 (R1)	148.6	823
2	EDG2INCMVP2 (R1)	194.8	823
3	MVP4 (31BBE11) (R2)	277	1645
4	31BBE11 (INC FROM EDG) (R3)	277	1645
5	31BBE10 (TIE TO 33BBE06) (R4)	277	1645
6	33BBE06 (TIE TO 31BBE10) (R5)	277	1645

The short-circuit simulation used a symmetrical three-phase fault placed at BUS33. A three-phase fault was selected because it produces the highest fault current for evaluating the phase OCR functions 50/51P. Ground-fault relays are outside the scope of this study because earth-fault protection is handled by different relay functions, such as 50N/51N or 50G/51G.

The coordination analysis was limited to one fault-location scenario, namely BUS33. The optimization model consists of five setting groups. R1 is a common setting applied identically to EDG1INCMVP1 and EDG2INCMVP2. Because both incoming relays observe a fault current of 823 A and use the same characteristic curve, pickup current, and TDS, they are modeled with identical operating times and trip simultaneously. The remaining groups are mapped as R2 = MVP4 (31BBE11), R3 = 31BBE11 (INC FROM EDG), R4 = 31BBE10 (TIE TO 33BBE06), and R5 = 33BBE06 (TIE TO 31BBE10). Therefore, the operating sequence from the relay closest to the fault toward the backup relays is R5, R4, R3, R2, and R1. The fault-current vector used in MATLAB is [823, 1645, 1645, 1645, 1645] A for R1 through R5; R1 is counted once as the common stage of the two incoming relays.

The pickup current is not an optimization variable but a fixed input based on the latest relay settings. The R1 setting is jointly applied to EDG1INCMVP1 and EDG2INCMVP2 using a CT ratio of 300/1 A and a secondary pickup of 0.83 A, yielding an R1 primary pickup of 249.00 A. R2 through R5 use a primary pickup of 296.39 A. Therefore, the existing, AMFA, and PSO settings use the same pickup vector, [249.00; 296.39; 296.39; 296.39; 296.39] A, while TDS is the optimization variable.

F. OCR Coordination Optimization Formulation

The optimization variables are the TDS values of five OCR setting groups. R1 is shared by the incoming relays of EDG1 and EDG2 and is represented by one variable because both relays operate simultaneously. For each TDS candidate, the operating time of every coordination stage is calculated using the IEC Normal Inverse curve. The basic objective-function component is the sum of the operating times of the five coordination stages; the identical R1 operating time of the two incoming relays is counted once to avoid double-counting simultaneous operation. A penalty is added only for primary-backup pairs with a CTI below the minimum limit of 0.3 s. The objective-function formulation must remain consistent with the technical coordination criteria so that reducing the operating time does not cause miscoordination [16].

$$\text{Fitness} = \text{SUM}(i = 1 \text{ to } N)\ t_i + P$$

For coordination pair k, CTI_k is calculated as t_backup,k - t_primary,k. MATLAB calculates the operating times, CTIs, and penalties using double precision; the table values are rounded only for presentation. The penalty is accumulated for each CTI violation using a coefficient K of 10,000,000. If all CTIs satisfy the minimum limit, every penalty component is zero and the fitness equals the sum of the relay operating times.

$$P = K\ \text{SUM}(k = 1 \text{ to } m)\ [\max(0, \text{CTI_min} - \text{CTI_k})]^2$$

Table IV lists the primary-backup relay pairs used as the basis for calculating the CTI during optimization.

TABLE IV. COORDINATION PAIRS AMONG RELAY-SETTING GROUPS

Pair	Primary Relay	Backup Relay
1	R5	R4
2	R4	R3
3	R3	R2
4	R2	R1 (EDG1 and EDG2)

G. AMFA and PSO Parameters and Optimization Procedures

The optimization was performed for five TDS variables bounded between 0.05 and 1.20, with a minimum CTI of 0.3 s. AMFA and PSO were each executed for 30 runs using a population of 30 candidates and 100 iterations per run. The initial TDS values were generated randomly from a uniform distribution within these limits. Both algorithms used the same fault-current data, pickup currents, relay pairs, objective function, and penalty coefficient K of 10,000,000. Equal population sizes, iteration counts, run counts, and system inputs formed the basis of the benchmark scenario. The number of function evaluations was not used as a stopping criterion because AMFA and PSO have different update structures.

AMFA used 30 fireflies, beta0 = 1, and gamma = 1. Attractiveness was calculated as beta = beta0 exp(-gamma r_ij^2), where r_ij is the distance between fireflies i and j. The randomization parameter was adapted according to alpha(iter) = alpha_min + (alpha0 - alpha_min)(1 - iter/MaxIter), with alpha0 = 0.25 and alpha_min = 0.01. Through this mechanism, larger random steps at the beginning support exploration, while the gradual reduction strengthens exploitation near the best solution. A firefly with worse fitness moves toward a firefly with better fitness, after which each TDS value is restricted to the specified range.

PSO used 30 particles with an inertia weight w = 0.7, a cognitive coefficient c1 = 2, and a social coefficient c2 = 2. The initial velocity of each particle was set to zero.

At each iteration, the velocity was updated from the inertia, personal-best, and global-best components; the particle position was then updated and restricted to the TDS range of 0.05 to 1.20. PSO was used as the benchmark method with the same system inputs and fitness formulation as AMFA [17]. Applications of PSO and its hybrid variants to relay coordination show that the search for setting parameters can be directed toward minimizing the total operating time while satisfying the coordination constraints [18].

The stopping criterion for both algorithms was completion of 100 iterations; the program used neither early stopping nor an equal-function-evaluation limit. In PSO, the fitness is evaluated once for each particle at every iteration. In AMFA, the fitness is evaluated when a firefly moves toward a firefly with better fitness within the i-j pairwise loop; consequently, the actual number of function evaluations may differ from that of PSO. This difference is acknowledged as a limitation of the comparison, and the results are not used to claim computational-efficiency superiority for either algorithm. To ensure reproducibility, the random seed was set using rng(run), so runs 1 through 30 used seeds 1 through 30. The best-so-far value was stored at each iteration, and the feasibility of the final solution was determined by whether all minimum CTIs were satisfied.

III. Results and Discussion

A. System Modeling Results

For the scenario with one active load, the total generation is 2.5686 MW and 1.6072 MVAr, equivalent to 3.0300 MVA at an overall power factor of 84.77%. Lump5 absorbs 2.5373 MW and 1.5725 MVAr, or 2.9851 MVA at a power factor of 85.00%. The system losses are 0.0313 MW and 0.0347 MVAr. Power balance is satisfied because 2.5373 + 0.0313 = 2.5686 MW and 1.5725 + 0.0347 = 1.6072 MVAr. Thus, the total supply is not obtained by directly adding the MVA magnitudes of EDG1 and EDG2, but from the resultant total active and reactive powers.

TABLE V. SUMMARY OF EDG BLACKSTART SYSTEM LOAD-FLOW RESULTS

Object	P (MW)	Q (MVAr)	S (MVA)	PF (%)
EDG1	0.4436	1.5591	1.6210	27.37
EDG2	2.1250	0.0481	2.1255	99.97
Total generation	2.5686	1.6072	3.0300	84.77
Lump5 (3 MVA rating)	2.5373	1.5725	2.9851	85.00
System losses	0.0313	0.0347	0.0467	-

The load-flow bus voltages range from 98.75% to 99.58% of the nominal voltage. At a nominal voltage of 6.3 kV, a bus voltage of 98.75% is approximately 6.22 kV. The branch voltage drops range from 0.4% to 0.8%. These results indicate that the voltage profile is suitable as the initial condition for the short-circuit and OCR coordination studies.

The three-phase fault simulation at BUS33 shows that EDG1INCMVP1 and EDG2INCMVP2 each observe a fault current of 823 A. Because both use the same setting, the two incoming relays are represented by R1 and are modeled to trip simultaneously. R2 through R5 each observe a fault current of 1645 A. The current difference between the R1 stage and the downstream relays results from the relay locations and the division of the current contributions along the system path, although all values correspond to the same fault-location scenario. The current data for each setting group used in the optimization are presented together with the primary pickup, PSM, TDS, and operating time in Table IX to permit reproduction of the calculations.

B. Analysis of Existing Relay Settings

The existing relay settings are used as the initial condition or baseline. The existing data include the current-transformer (CT) ratios, pickup currents on the relay secondary side, their conversion to primary amperes, and the Time Dial Settings (TDS). All CTs in Table VI have a nominal secondary current of 1 A, and all relays use the IEC Normal Inverse curve. Distinguishing the secondary and primary units is necessary to prevent the pickup value from being confused with the primary current used to calculate the Plug Setting Multiplier (PSM).

TABLE VI. CT RATIOS, PICKUP CURRENTS, AND EXISTING RELAY TDS VALUES

Relay	CT Ratio	Secondary Pickup Used (A)	Primary Pickup Used (A)	Existing TDS
R1*	300/1 A	0.830	249.00	0.50
R2	800/1 A	0.37049	296.39	0.50
R3	125/1 A	2.37112	296.39	0.50
R4	125/1 A	2.37112	296.39	0.50
R5	800/1 A	0.37049	296.39	0.50

The R1* designation in Table VI indicates the common setting group applied identically to EDG1INCMVP1 and EDG2INCMVP2. With a 300/1-A CT and a secondary pickup of 0.83 A, the primary pickup of R1 is 249.00 A. R2 and R5 use 800/1-A CTs, whereas R3 and R4 use 125/1-A CTs; the primary pickup used in the calculation is 296.39 A. The corresponding secondary values are approximately 0.37049 A for a 800/1-A CT and 2.37112 A for a 125/1-A CT. The displayed settings may be rounded to 0.37 A and 2.37 A, but MATLAB consistently uses a primary pickup of 296.39 A. All setting groups use an existing TDS of 0.50.

Comparison with the load-flow results shows that the EDG1INCMVP1 current of 148.6 A is 100.4 A, or 40.32%, below the R1 pickup of 249 A. The EDG2INCMVP2 current of 194.8 A is also 54.2 A, or 21.77%, below the R1 pickup. Thus, the common R1 pickup is above the normal operating currents of both EDGs. For R2 through R5, the load-flow current of 277 A is 19.39 A, or 6.54%, below the pickup of 296.39 A.

After the existing pickup and TDS values are entered, the existing TCCs can be generated in ETAP. These curves are then used to determine whether the initial relay coordination satisfies the minimum CTI or whether overlap remains between the relay curves.

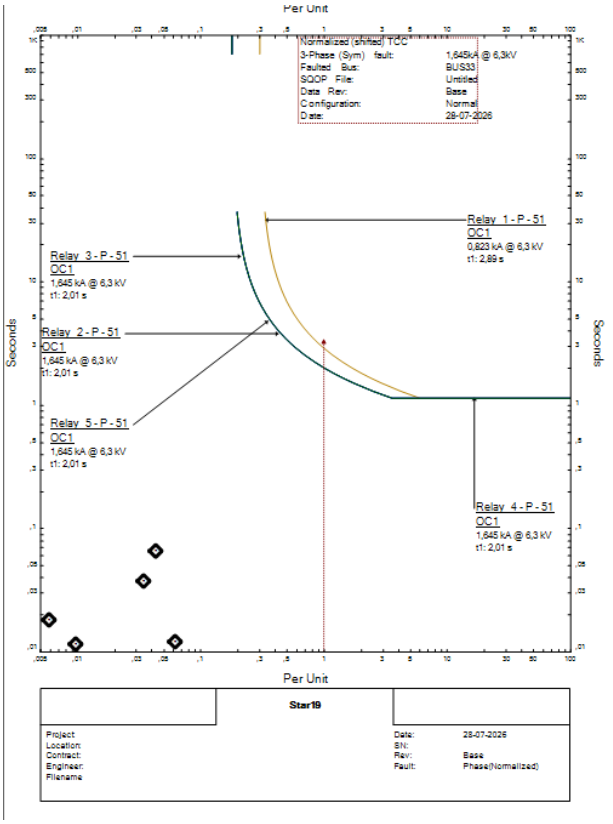


Fig. 2 is used as the reference for evaluating relay coordination before optimization.

Fig. 2. TCCs of the Existing Relay Settings

As a quantitative baseline, the operating times of the existing settings were calculated using the IEC Normal Inverse equation, the BUS33 fault currents in Table III, the primary pickup currents in Table VI, and a TDS of 0.50. The full-precision values are t_R1 = 2.8927767191 s and t_R2 through t_R5 = 2.0074219975 s. The t_R1 value applies identically to EDG1INCMVP1 and EDG2INCMVP2, which trip simultaneously, but it is counted once as a common coordination stage. The CTIs for R5-R4, R4-R3, R3-R2, and R2-R1 are 0, 0, 0, and 0.8853547216 s, respectively. Thus, the three downstream pairs do not satisfy the minimum CTI of 0.3 s, whereas the R2-R1 pair does.

C. Optimization Results Using AMFA

AMFA optimization was performed for 30 runs to evaluate solution quality and consistency. Each run used a different random seed and produced one final fitness value. Dispersion statistics were calculated using the sample standard deviation with a divisor of n - 1. A smaller fitness indicates a shorter total relay operating time while the minimum CTI constraint remains satisfied.

TABLE VII. AMFA FITNESS RESULTS FOR 30 RUNS

Run	Fitness	Run	Fitness	Run	Fitness
1	4.065558	11	4.078708	21	4.093065
2	4.079267	12	4.090392	22	4.095146
3	4.086633	13	4.076451	23	4.076126
4	4.054961	14	4.063592	24	4.083844
5	4.086018	15	4.068231	25	4.083950
6	4.095752	16	4.071497	26	4.082140
7	4.100626	17	4.060600	27	4.103959
8	4.095228	18	4.076692	28	4.092115
9	4.100750	19	4.064544	29	4.087099
10	4.063570	20	4.106543	30	4.058496

As shown in Table VII, AMFA produced the best fitness of 4.054961 in run 4 and the worst fitness of 4.106543 in run 20. The narrow range indicates that most runs reached nearby regions of the solution space.

The mean AMFA fitness is 4.081385, with a sample standard deviation of 0.014481. The standard deviation was calculated from the 30 fitness values using a divisor of n - 1. The coefficient of variation of 0.35% indicates very small dispersion relative to the mean and therefore good consistency among the AMFA runs.

TABLE VIII. STATISTICS OF THE 30 AMFA RUNS

Parameter	Value
Best fitness	4.054961
Worst fitness	4.106543
Mean fitness	4.081385
Sample std. dev.	0.014481
CV	0.35%
Feasible rate	100%

All 30 AMFA runs satisfied the CTI constraints, yielding a feasible rate of 100%. The best AMFA solution also satisfied every minimum CTI of 0.3 s.

TABLE IX. FAULT CURRENT, PRIMARY PICKUP, PSM, TDS, AND OPERATING TIME OF THE BEST AMFA SOLUTION

R	I_fault (A)	I_pickup (primary A)	PSM	TDS	t (s)
R1	823	249	3.305221	0.246670	1.427121
R2	1645	296.39	5.550120	0.278412	1.117779
R3	1645	296.39	5.550120	0.200478	0.804887
R4	1645	296.39	5.550120	0.125642	0.504432
R5	1645	296.39	5.550120	0.050000	0.200742

The PSM values were calculated from the fault currents and primary pickup currents, which were used identically for all methods. The R1 group, which is common to EDG1INCMVP1 and EDG2INCMVP2, has a PSM of 823/249 = 3.305221. R2 through R5 use a pickup of 296.39 A, giving a PSM of 1645/296.39 = 5.550120. Substitution of the PSM and TDS values into the IEC Normal Inverse equation produces the operating times in Table IX. For the best solution, the CTIs for R5-R4, R4-R3, R3-R2, and R2-R1 are 0.3036895678 s, 0.3004557285 s, 0.3128914268 s, and 0.3093418321 s, respectively. All values satisfy the minimum CTI of 0.3 s.

Using the operating times of the best solution, the CTI was reproduced from CTI = t_backup - t_primary for the R5-R4, R4-R3, R3-R2, and R2-R1 pairs. The final pair represents the coordination of R2 with the R1 stage, which is applied identically to the incoming relays of EDG1 and EDG2. The resulting values are 0.3036895678 s, 0.3004557285 s, 0.3128914268 s, and 0.3093418321 s, respectively. These values are identical to those in Table XIII, and all satisfy the minimum CTI of 0.3 s.

D. Comparison with the Benchmark Method and Existing Settings

To strengthen the evaluation, the AMFA results were compared with PSO as a benchmark method. Both algorithms used the same system data, fitness function, TDS limits, population of 30 candidates, 100 iterations, 30 runs, and sequence of random seeds. Because the numbers of function evaluations were not equalized, the comparison focuses on fitness quality, run-to-run stability, and feasible rate under the same experimental

configuration, rather than claiming that one algorithm is computationally more efficient. In this study, PSO is used only as an additional benchmark and is not the primary focus.

TABLE X. STATISTICAL SUMMARY OF 30 AMFA AND PSO RUNS

Parameter	AMFA	PSO
Best fitness	4.054961	4.131915
Worst fitness	4.106543	13.263455
Mean fitness	4.081385	5.580949
Sample std. dev.	0.014481	2.585672
CV	0.35%	46.33%
Feasible rate	100%	100%

Table X shows that AMFA produced lower best and mean fitness values than PSO. The AMFA sample standard deviation and CV were also substantially smaller, while both algorithms achieved a feasible rate of 100%. Under the configuration of 30 candidates, 100 iterations, and 30 runs, AMFA achieved lower best and mean fitness values and less variation among runs than PSO.

Six of the 30 PSO runs produced high fitness values ranging from 9.550575 to 13.263455, whereas the other 24 runs ranged from 4.131915 to 4.907864. This dispersion resulted in a PSO sample standard deviation of 2.585672 and a CV of 46.33%. By contrast, all AMFA fitness values were between 4.054961 and 4.106543.

The convergence curve in Fig. 3 was constructed from the mean best fitness at each iteration across 30 runs. A logarithmic scale was used because the initial PSO fitness was very large owing to penalties applied to candidates that violated the CTI, allowing the progress of both algorithms to remain visible on one graph.

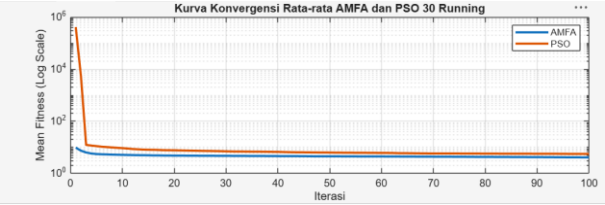


Fig. 3. Mean Convergence Curves of AMFA and PSO over 30 Runs on a Logarithmic Scale

Fig. 3 presents a comparison of the convergence characteristics of the two algorithms during the optimization process. Fig. 3 shows that AMFA is already in a lower-fitness region during the early iterations and then decreases gradually toward its final value. PSO decreases sharply in the initial iterations as penalized solutions are discarded, but its final mean fitness remains higher. This pattern is consistent with the final mean fitness values of 4.081385 for AMFA and 5.580949 for PSO.

Table XI presents the changes in TDS for each relay among the existing settings, the AMFA results, and the PSO benchmark.

TABLE XI. COMPARISON OF EXISTING AND OPTIMIZED SETTINGS

Relay	Existing TDS	AMFA TDS	Benchmark TDS (PSO)	Remarks
R1	0.50	0.2467	0.2514	AMFA is lower than the existing and PSO settings while satisfying the CTI.
R2	0.50	0.2784	0.2826	AMFA is lower than the existing and PSO settings while satisfying the CTI.
R3	0.50	0.2005	0.2064	AMFA is lower than PSO while satisfying the CTI.
R4	0.50	0.1256	0.1270	AMFA is lower than PSO while satisfying the CTI.
R5	0.50	0.0500	0.0509	AMFA reaches the minimum TDS limit while satisfying the CTI.

Table XII compares the operating times, CTIs, penalties, fitness values, and coordination-feasibility status of the three settings analyzed.

TABLE XII. PERFORMANCE COMPARISON OF EXISTING, PSO, AND AMFA SETTINGS

Parameter	Existing	PSO	AMFA
t R1 (s)	2.892777	1.454619	1.427121
t R2 (s)	2.007422	1.134437	1.117779
t R3 (s)	2.007422	0.828655	0.804887
t R4 (s)	2.007422	0.509966	0.504432
t R5 (s)	2.007422	0.204238	0.200742
Total time, SUM t (s)	10.922465	4.131915	4.054961
CTI R5-R4 (s)	0.000000	0.305729	0.303690
CTI R4-R3 (s)	0.000000	0.318688	0.300456
CTI R3-R2 (s)	0.000000	0.305783	0.312891
CTI R2-R1 (s)	0.885355	0.320182	0.309342
CTI violations	3	0	0
Penalty	2,700,000.000000	0	0
Fitness	2,700,010.922465	4.131915	4.054961
Reduction in SUM t	0.00%	62.17%	62.88%
Status	Not feasible	Feasible	Feasible

Table XII presents rounded operating times and CTIs for readability, whereas the penalty was calculated using the full-precision values. For the existing settings, the total operating time is 10.9224647091 s and the full-precision CTI vector is [0; 0; 0; 0.8853547216] s. With K = 10,000,000, three CTI violations of 0.3 s each produce a penalty of 2,700,000.000000. The existing-setting fitness is therefore 10.9224647091 + 2,700,000.000000 = 2,700,010.922465. For the best PSO and AMFA solutions, all CTIs satisfy the minimum limit, so the penalty is zero and the fitness equals the sum of the relay operating times.

Compared with the existing settings, which use the same pickup currents as the optimization methods, PSO reduces the total operating time by 62.17%, whereas AMFA reduces it by 62.88%. AMFA provides a total operating time 0.076954 s lower than PSO and eliminates the three coordination violations present in the existing settings. Therefore, the existing, PSO, and AMFA settings are compared using identical pickup-current inputs.

E. CTI Analysis

The CTI analysis verifies that every primary-backup relay pair satisfies the minimum limit of 0.3 s. Operating times are presented to ten decimal places so that the fitness components can be reproduced and directly compared with the MATLAB output.

TABLE XIII. CTI ANALYSIS AND FITNESS VERIFICATION OF THE BEST AMFA SOLUTION

Pair	t Primary (s)	t Backup (s)	CTI (s)	Status
R5-R4	0.2007421997	0.5044317675	0.3036895678	Satisfied
R4-R3	0.5044317675	0.8048874960	0.3004557285	Satisfied
R3-R2	0.8048874960	1.1177789228	0.3128914268	Satisfied
R2-R1	1.1177789228	1.4271207549	0.3093418321	Satisfied

The operating-time components summed in the objective function are t_R1 = 1.4271207549 s, t_R2 = 1.1177789228 s, t_R3 = 0.8048874960 s, t_R4 = 0.5044317675 s, and t_R5 = 0.2007421997 s. The t_R1 value is the common stage of EDG1INCMVP1 and EDG2INCMVP2, which operate simultaneously, and is therefore counted once. The sum of the operating times of the five stages is 4.0549611410 s. All CTI values in Table XIII exceed 0.3 s; therefore, P = 0 and the fitness is 4.0549611410.

F. TCC Analysis

The existing TCCs represent the initial relay-coordination condition before optimization. Under the existing settings, all relays use a TDS of 0.5, resulting in relatively long operating times. This condition provides the basis for evaluating the effect of AMFA optimization on relay operating speed and the arrangement of the primary-backup coordination.

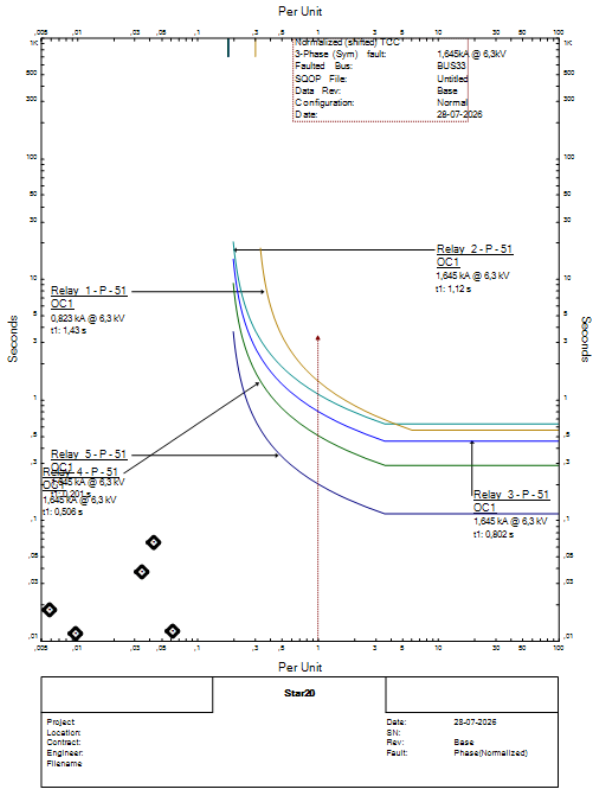


Fig. 4. TCCs Obtained from AMFA Optimization

Fig. 4 is presented to show the arrangement of the TCCs after the TDS values were optimized using AMFA. Fig. 4 shows the TCCs obtained after AMFA optimization.

The AMFA TCCs were generated using the latest primary pickup currents and TDS values. The R1 curve applies identically to the incoming relays of EDG1 and EDG2, so the two relays trip simultaneously. All relay pairs satisfy the minimum CTI of 0.3 s: 0.3037 s for R5-R4, 0.3005 s for R4-R3, 0.3129 s for R3-R2, and 0.3093 s for R2-R1. Thus, AMFA accelerates relay operation without sacrificing coordination selectivity.

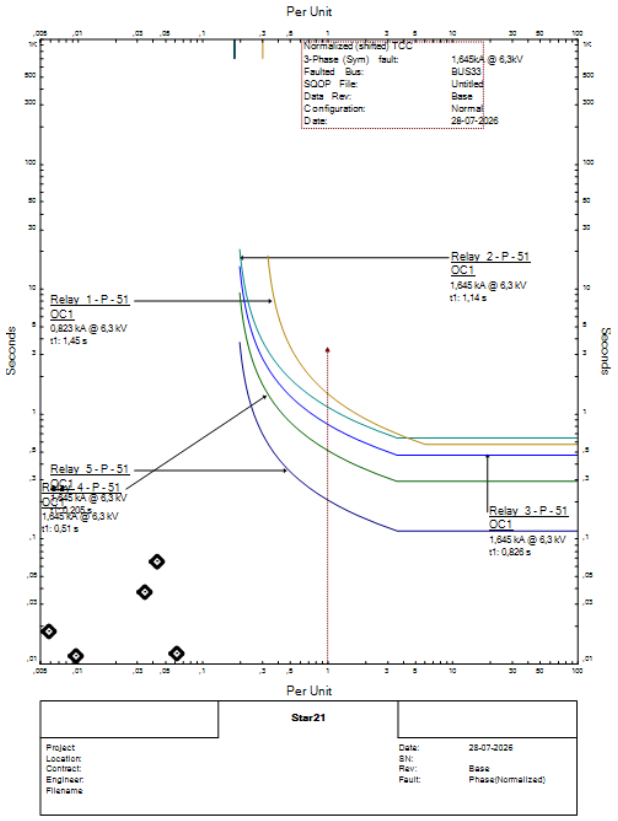


Fig. 5. TCCs Obtained from PSO Optimization

Fig. 5 presents the TCCs obtained from PSO optimization as a benchmark for the AMFA results. Fig. 5 shows the PSO optimization results used as a benchmark for AMFA.

The PSO TCCs in Fig. 5 are used as the benchmark for the AMFA results. All relay pairs in the best PSO solution satisfy the minimum CTI of 0.3 s: 0.3057 s for R5-R4, 0.3187 s for R4-R3, 0.3058 s for R3-R2, and 0.3202 s for R2-R1. The total PSO operating time is 4.131915 s, slightly higher than the AMFA total operating time of 4.054961 s.

G. Advantages of AMFA in the EDG Blackstart System

The advantage of AMFA in this study is evident from its fitness quality and the stability of the results over 30 runs. The mean AMFA fitness of 4.081385 is lower than the PSO value of 5.580949. The AMFA sample standard deviation of 0.014481 and CV of 0.35% are also substantially smaller than the PSO sample standard deviation of 2.585672 and CV of 46.33%. Both algorithms achieved a feasible rate of 100%. These results indicate that AMFA is more consistent in obtaining solutions with a low total operating time.

The characteristics of the EDG Blackstart system also affect the difficulty of the optimization problem. Because the fault sources are limited-capacity synchronous generators, the fault current is lower than in a grid-connected system. The PSM values observed by the relays are relatively close; consequently, small TDS changes can significantly affect the CTI. Under these conditions, the algorithm requires a strong search capability to identify a TDS combination that is both fast and selective.

AMFA has an adaptive mechanism that helps balance global and local searches. During the early stages, the algorithm explores the solution space to avoid local

optima. In the subsequent stages, the search becomes more focused on the region of the best solution. This mechanism enables AMFA to produce solutions that are not only good in one run but also consistent across multiple runs.

These results are not intended to claim the discovery of a new AMFA structure. The demonstrated contribution is the effectiveness of applying AMFA adapted from [11] to a field case involving the EDG Blackstart system, with pickup limits, CTI requirements, and relay configurations defined by the actual system. Therefore, the reported advantages are limited to the BUS33 scenario and the parameters used in this study; generalization to other fault locations or operating configurations requires further testing.

This study is limited to the operating configuration and the three-phase fault scenario at BUS33. Therefore, the results have not been generalized to all fault locations or changes in the EDG operating configuration. Future studies may evaluate additional fault locations and operating conditions.

Overall, the results show that AMFA is suitable for OCR coordination optimization in the radial EDG Blackstart system at the Muara Tawar Combined Cycle Power Plant. PSO remains useful as a benchmark, but the main focus is the application of AMFA to the existing system and the demonstration that its optimized settings provide faster, selective, and stable coordination. The comparison is limited to equal population and iteration configurations; this study does not claim computational-efficiency superiority because the numbers of function evaluations for the two algorithms were not equalized.

IV. Conclusion

This study optimized Overcurrent Relay coordination in the radial EDG Blackstart network at the Muara Tawar Combined Cycle Power Plant using the Adaptive Modified Firefly Algorithm. The system was modeled in ETAP to obtain load-flow data and three-phase short-circuit currents, while the optimization was performed in MATLAB. The optimized variables were the Time Dial Settings of five OCR setting groups using the IEC Normal Inverse characteristic and a minimum CTI of 0.3 s. The R1 group was applied identically to the incoming relays of EDG1 and EDG2; therefore, the two relays were modeled to trip simultaneously.

The load-flow results show that only Lump5, rated at 3 MVA, was active and consumed 2.5373 MW and 1.5725 MVAr, or 2.9851 MVA at a power factor of 85.00%. EDG1 supplied 0.4436 MW and 1.5591 MVAr, whereas EDG2 supplied 2.1250 MW and 0.0481 MVAr. The total system losses were 0.0313 MW and 0.0347 MVAr, while the bus voltages ranged from 98.75% to 99.58%. For the three-phase BUS33 fault scenario, the incoming relays of EDG1 and EDG2 each observed 823 A and were jointly represented as R1, whereas R2 through R5 each observed 1645 A.

The existing settings used a TDS of 0.5 for all setting groups, with an R1 pickup of 249 A and pickups of 296.39 A for R2 through R5. The best AMFA solution from 30 runs produced TDS values of 0.2467, 0.2784, 0.2005, 0.1256, and 0.0500 for R1 through R5, respectively. All relay pairs satisfied the minimum CTI: 0.3037 s for R5-R4, 0.3005 s for R4-R3, 0.3129 s for R3-R2, and 0.3093 s for R2-R1.

Over 30 runs, AMFA achieved a best fitness of 4.054961, a mean fitness of 4.081385, a sample standard deviation of 0.014481, a CV of 0.35%, and a feasible rate of 100%. PSO achieved a best fitness of 4.131915, a mean fitness of 5.580949, a sample standard deviation of 2.585672, a CV of 46.33%, and a feasible rate of 100%. AMFA produced better solution quality and stability and reduced the total operating time by 62.88% relative to the existing settings.

References

[1] M. P. Marbun, H. Atma, A. S. Surya, and I. Savitri, "Study of stochastic approach to determine value of lost load in Jawa-Madura-Bali system," in Proc. 4th Int. Conf. High Voltage Engineering and Power Systems (ICHVEPS), 2023, pp. 471-475, doi: 10.1109/ICHVEPS58902.2023.10257513. https://doi.org/10.1109/ICHVEPS58902.2023.10257513

[2] M. P. Marbun and P. D. Putra, "Adaptive defense scheme implementation in Muarakarang subsystem to prevent island operation failure," in Proc. 11th Electrical Power, Electronics, Communications, Control, and Informatics Seminar (EECCIS), 2022, pp. 88-93, doi: 10.1109/EECCIS54468.2022.9902921. https://doi.org/10.1109/EECCIS54468.2022.9902921

[3] J. L. Blackburn and T. J. Domin, Protective Relaying: Principles and Applications, 4th ed. Boca Raton, FL: CRC Press, 2014. https://doi.org/10.1201/b16518

[4] J. Muslim, D. F. Dakhlan, T. Kurnianto, D. R. Jintaka, and A. Amiruddin, "Isolated hybrid system protection performance: A study case in Island S," in Proc. Int. Conf. Technology and Policy in Energy and Electric Power (ICT-PEP), 2024, pp. 24-27, doi: 10.1109/ICT-PEP63827.2024.10733489. https://doi.org/10.1109/ICT-PEP63827.2024.10733489

[5] F. G. Savio, M. Pujiantara, and N. K. Aryani, "Optimasi koordinasi sistem proteksi inverse-time over current relay pada sistem distribusi radial dengan pertimbangan distributed generator untuk studi kasus area Lahat, Sumatera Selatan," Jurnal Teknik ITS, vol. 10, no. 2, 2021. https://doi.org/10.12962/j23373539.v10i2.67002

[6] A. Draz, M. M. Elkholy, and A. El-Fergany, "Over-current relays coordination including practical constraints and DGs: Damage curves, inrush, and starting currents," Sustainability, vol. 14, p. 2761, 2022. https://doi.org/10.3390/su14052761

[7] J. Ehrenberger and J. Svec, "Directional overcurrent relays coordination problems in distributed generation systems," Energies, vol. 10, no. 10, art. no. 1452, 2017, doi: 10.3390/en10101452. https://doi.org/10.3390/en10101452

[8] J. Arifin, M. P. Marbun, and T. Nur, "Analisis keandalan subsistem kelistrikan Madura dengan simulasi beban dan kontingensi," Master's thesis, Institut Teknologi PLN, Jakarta, Indonesia, 2025.

[9] F. Korib, P. Pawenary, and R. Yasser, "Optimalisasi relai berbasis protokol IEC 61850 dalam pengembangan relai adaptif proteksi busbar Gardu Induk 70 kV Indramayu," Master's thesis, Institut Teknologi PLN, Jakarta, Indonesia, 2024.

[10] M. Irfan, A. Wadood, T. Khurshaid, B. M. Khan, K.-C. Kim, S.-R. Oh, and S.-B. Rhee, "An optimized adaptive protection scheme for numerical and directional overcurrent relay coordination using Harris Hawk Optimization," Energies, vol. 14, no. 18, art. no. 5603, 2021, doi: 10.3390/en14185603.
https://doi.org/10.3390/en14185603

[11] A. Tjahjono, D. O. Anggriawan, A. K. Faizin, A. Priyadi, M. Pujiantara, T. Taufik, and M. H. Purnomo, "Adaptive modified firefly algorithm for optimal coordination of overcurrent relays," IET Generation, Transmission & Distribution, vol. 11, no. 10, pp. 2575-2585, 2017. https://doi.org/10.1049/iet-gtd.2016.1563

[12] A. Y. Abdelaziz, E. S. Ali, and S. M. Abd Elazim, "Optimal coordination of overcurrent relays using modified firefly algorithm," Electric Power Components and Systems, vol. 44, no. 15, pp. 1695-1709, 2016. https://doi.org/10.1080/15325008.2015.1117540

[13] S. D. Saldarriaga-Zuluaga, J. M. Lopez-Lezama, and N. Munoz-Galeano, "Optimal coordination of over-current relays in microgrids considering multiple characteristic curves," Alexandria Engineering Journal, vol. 60, no. 2, pp. 2093-2113, 2021, doi: 10.1016/j.aej.2020.12.012. https://doi.org/10.1016/j.aej.2020.12.012

[14] IEC, IEC 60255: Measuring Relays and Protection Equipment. Geneva: International Electrotechnical Commission, 2009.

[15] Siemens, SIPROTEC 5 7SJ82 Overcurrent Protection Relay Manual. Siemens AG.

[16] S. D. Godwal, K. S. Pandya, S. C. Vora, C. R. Mehta, and V. R. Rajput, "Optimal overcurrent relay coordination for interconnected power systems: A proper approach and improved technique," e-Prime - Advances in Electrical Engineering, Electronics and Energy, vol. 5, art. no. 100248, 2023, doi: 10.1016/j.prime.2023.100248. https://doi.org/10.1016/j.prime.2023.100248

[17] R. Eberhart and J. Kennedy, "A new optimizer using particle swarm theory," in Proceedings of the Sixth International Symposium on Micro Machine and Human Science, pp. 39-43, 1995. https://doi.org/10.1109/MHS.1995.494215

[18] Y. Wang, K. Habib, A. Wadood, and S. Khan, "The hybridization of PSO for the optimal coordination of directional overcurrent protection relays of the IEEE bus system," Energies, vol. 16, no. 9, art. no. 3726, 2023, doi: 10.3390/en16093726.
https://doi.org/10.3390/en16093726